

# Self-interaction Corrected Local Spin Density Theory of 5f Electron Localization in Actinides

A. Svane,<sup>1</sup> L. Petit,<sup>2</sup> Z. Szotek,<sup>3</sup> and W. M. Temmerman<sup>3</sup>

<sup>1</sup>*Department of Physics and Astronomy, University of Aarhus, DK-8000 Aarhus C, Denmark*

<sup>2</sup>*Computer Science and Mathematics Division, and Center for Nanophase Materials Sciences, Oak Ridge National Laboratory, Oak Ridge, Tennessee 37831, USA*

<sup>3</sup>*Daresbury Laboratory, Daresbury, Warrington WA4 4AD, United Kingdom*

(Dated: September 1, 2018)

The electronic structures of the actinide elements U, Np, Pu, Am, Cm and Bk are investigated within the self-interaction corrected local spin density approximation. This method allows to describe a dual character of the 5f electrons, some of which occupy localized and core-like states, while the remaining 5f electrons hybridize and form bands. Based on energetics the calculations predict delocalization/paramagnetism in the early actinides, and localization/anti-ferromagnetism in the later actinides. The corresponding calculated equilibrium volumes are in agreement with the experimental values. For Pu and Am, the method wrongly predicts magnetic ordering, but we find that the paramagnetic state gives a better description of cohesive properties. Under compression, in the later actinides, a localization-delocalization transition happens gradually as more and more f electrons become band-like with decreasing volume. Pu is already at this transition point at ambient conditions. Delocalization sets in for Am and Bk at a compression of  $V \sim 0.75V_0$ , for Cm at  $V \sim 0.60V_0$ , where  $V_0$  is the equilibrium volume, and the transition is complete for  $V \sim 0.4 - 0.5V_0$  in these three elements.

PACS numbers: 71.15.Nc, 71.27.+a, 71.30.+h, 71.23.An

## I. INTRODUCTION

The electronic structure of actinides remains an active area of research both experimentally<sup>1,2,3,4,5,6,7,8,9,10,11,12</sup> and theoretically.<sup>13,14,15,16,17,18,19,20,21,22,23,24,25,26,27,28,29,30,31</sup> The intricate nature of the f-electrons, their sensitivity to external probes, like temperature and pressure, and their magnetic ordering are at the center of interest. Already in the seventies it emerged that with respect to volume behaviour one had to distinguish between the early actinide elements, with their bonding properties resembling those of the transition metals, and the late actinides, where the lattice parameters remain relatively unchanged, reminiscent of the localized f-states of the rare earth series.<sup>4</sup> Pu is on the border line between these two opposing pictures with a particularly rich phase diagram.<sup>5</sup> These trends observed across the actinide series can be correlated with an increase of the on-site Coulomb correlation energy of the f-electrons which gradually conquers the band formation energy as one progresses through the series. With applied external pressure the late actinides exhibit volume collapses associated with structural phase transitions signaling the onset of f-bonding.<sup>6</sup>

Most theoretical studies on the actinide elements<sup>13,14,15,16,17,18,19,20,21,22,23,24,25,26,27,28,29,30,31,32</sup> are based on density functional theory (DFT), in either its local density or generalized gradient approximation, and their overall conclusion is that the early actinides, Th, Pa, U, and Np, are well described by the conventional band theory, as their f-electrons contribute to bonding, and the equilibrium structures and lattice

parameters are in good agreement with experiments.<sup>13</sup> However, for the later actinides the band picture fails, and additional assumptions or parameters derived from experiments need to be invoked, diminishing the predictive power of the approach. Thus, from Cm to Es, the lattice parameters are found to be in better agreement with experiment when the f-electrons are prevented from participating in bonding,<sup>14</sup> indicating the need of a different energy functional. For Pu and Am, situated at the localization-delocalization transition, neither of these two approaches is capable of describing their electronic and magnetic properties, in particular conventional band theory finds both Am and  $\delta$ -Pu magnetic. The onset of spin-polarization in band theory may be interpreted as a signature of f-electron localization,<sup>15</sup> albeit only close to half-filling, and when combined with anti-ferromagnetic ordering and orbital polarization<sup>16,17,18</sup> a quite accurate account of bonding energetics is obtained. The predicted magnetic ordering is however in disagreement with the experimentally observed Pauli enhanced paramagnetic ground state in  $\delta$ -Pu and Am. By allowing for a complete disorder of the local magnetic moments, Niklasson et al.<sup>19</sup> obtained a reasonably accurate description of bond lengths and bulk moduli throughout the actinide series, however, the underlying assumption of fluctuating local moments has not been confirmed by experiments.

The inadequacy of the local density functional for the later actinides can be traced to its inaccurate representation of strong electron-electron interaction, which tends to localize the f-electrons on their atomic sites. To overcome this shortcoming, all implementations of the LDA+U approach<sup>20,21,22,23</sup> introduce the effective

Coulomb  $U$  parameter that separates the  $f$ -manifold into lower and upper Hubbard bands, and removes  $f$ -degrees of freedom from the Fermi level. In the fully localized limit (FLL) LDA+ $U$  finds  $\delta$ -Pu magnetic,<sup>20,21,23</sup> but a careful balancing of spin-orbit and exchange interactions in the implementation of Ref. 22 leads to a non-magnetic ground state of  $\delta$ -Pu. In the around mean-field (AMF) flavour of LDA+ $U$  non-magnetic ground states were found for both  $\delta$ -Pu and Am.<sup>23,32</sup> The recent development of dynamical mean-field theory (DMFT),<sup>33</sup> combined with the LDA+ $U$  approach, has enriched the field in terms of phenomena accessible to calculations, including both ground state cohesion,<sup>24</sup> phonons<sup>25</sup> and photoemission.<sup>26,27,34</sup> However, most applications to date invoke the Hubbard Hamiltonian and inherit the uncertainties associated with the LDA+ $U$  method, most notably the effective  $U$  and the double counting correction, shortcomings that might be overcome if DMFT could be successfully merged with the GW technique.<sup>35</sup> The disordered local moment approach of Ref. 19 is related to DMFT by a static approximation.

The self-interaction corrected local spin density (SIC-LSD) theory<sup>31</sup> provides a dual picture of coexisting localized and band-like  $f$ -electrons, which was also conjectured<sup>30</sup> to be the appropriate picture of the  $\delta$ -phase of Pu. The method is fully ab-initio as both kinds of  $f$ -electrons are treated on an equal footing, with no adjustable parameters. Consequently, a unique total energy functional can be applied to the entire range of actinide elements to determine the ground state localized/delocalized  $f$ -electron manifold of each element. The method was previously applied to the actinide elements Pu to Cf assuming a ferromagnetic ground state and, with the exception of Pu, the calculated volumes and bulk moduli were in reasonably good agreement with the experimental values.<sup>31</sup> The motivation for the present paper is to extend the SIC-LSD study to other magnetic orderings (para-, ferro- and antiferro-magnetism), and explore the consequences for the bonding properties and valence state of the actinides. In addition, the delocalization of  $f$ -electrons under pressure in the later actinides is also investigated. Through the present more comprehensive study, we seek to establish and document the SIC-LSD applicability and status regarding a thorough physical understanding of such complex systems as actinides.

The magnetic and paramagnetic states are realized by switching on or off the spin dependent part of the exchange-correlation potential. We find that, except for U and Np, the spin-polarized solution has always a lower energy than the non-magnetic solution, which in case of Pu and Am is in disagreement with experimental observation. However, it emerges that assuming a paramagnetic representation of the localized states provides a much improved description of the equilibrium volumes of both  $\delta$ -Pu and Am. Antiferromagnetic order is found to be the lowest energy solution for both Cm and Bk, in agreement with experiment, providing slightly improved

specific volumes compared to the values calculated for the ferromagnetic case. Since SIC-LSD describes well the delocalized nature of the  $f$ -electrons in the early actinides and the localized nature of the  $f$ -electrons in the late actinides, this demonstrates that the transition from  $f$ -bonding to  $f$ -localization in the  $5f$  series is reproduced, while an adequate description of the cross-over region depends strongly on the representation used for the localized states.

The paper is organized as follows. In Section II the important aspects of the SIC-LSD method are outlined. In Section III we present our results for the U, Np, Pu, Am, Cm and Bk metals. The observed trends of the present study are discussed in Section IV, and Section V gives our conclusions.

## II. THEORY

### A. The SIC-LSD total energy method

The LSD approximation to exchange and correlation introduces an unphysical interaction of the electron with itself,<sup>36</sup> which, though insignificant for extended band states, may lead to uncontrollable errors in the description of atomic-like localized states, for example the  $f$ -electrons in the later actinides. The SIC-LSD method<sup>37,38,39</sup> corrects for this self-interaction, by postulating a manifold of coexisting localized and delocalized  $f$ -electrons, and by adding to the LSD total energy functional an explicit energy contribution for an electron to localize. The approach is fully ab-initio, as both localized and delocalized states are expanded in the same set of basis functions, and are thus treated on an equal footing.

One major advantage of the SIC-LSD energy functional is that it allows to realize and study different valence states of ions constituting a solid. By assuming atomic configurations with different total numbers of localized states, self-consistent minimization of the total energy leads to different local minima of the same total energy functional,  $E^{SIC-LSD}$ , and hence their total energies may be compared. The configuration with the lowest energy defines the ground state configuration. If no localized states are assumed,  $E^{SIC-LSD}$  coincides with the conventional LSD functional, *i.e.*, the Kohn-Sham minimum of the  $E^{LSD}$  functional is also a local minimum of  $E^{SIC-LSD}$ . Another advantage of the SIC-LSD scheme is the possibility to localize  $f$ -states of different symmetry. In the present work we exploit this possibility to investigate several magnetic structures including non-magnetic, ferromagnetic and antiferromagnetic order.

Given the total energy functional  $E^{SIC-LSD}$ , the computational procedure is as for the LSD case, *i.e.* minimization is accomplished by iteration until self-consistency. In the present work, the electron wavefunctions are expanded in linear-muffin-tin-orbital (LMTO) basis functions,<sup>40</sup> and the energy minimization problem

becomes a non-linear optimization problem in the expansion coefficients, which is only slightly more complicated for the SIC-LSD functional. Further details of the present implementation can be found in Ref. 37. For a variety of applications to  $d$  and  $f$  electron solids, see Refs. 37,41,42,43,44,45 and references therein.

The elementary excitations of solids, *i.e.* the one-particle energies, are often approximated by the band eigenenergies of the Kohn-Sham scheme, although a formal justification does not exist. Although for weakly correlated materials such an approximation may be reasonable, for localized electron states it is ill founded. It is possible to define band states constructed as Bloch combinations of the localized states (sometimes referred to as 'canonical orbitals'<sup>46</sup>), however the associated band energies bear little resemblance to physical removal energies, as *e.g.* observed in photoemission spectroscopy. This is in contrast to the LDA+ $U$  approach where better agreement with photoemission experiment can be accomplished by an appropriate choice of the  $U$  parameter and double-counting correction. On the other hand, the SIC-LSD method, being fully *ab-initio*, does not require parameters, and can therefore be applied to study trends in energetics of the entire series of actinides in a comprehensive manner, and with potentially predictive capability. The SIC-LSD method is not a means to explain spectroscopies but should be treated as a useful total energy approach, allowing to study a variety of phenomena and among them valences and valence transitions.

## B. Computational Details

Calculations have been performed for the face-centered cubic (fcc), hexagonal close-packed (hcp), and double hexagonal close-packed (dhcp) crystal structures. The Wannier states describing the localized  $f$  electrons are expanded on clusters of 32, 64 or 48 sites around the localization site,<sup>38</sup> for these three cases. Similarly, the itinerant states have been sampled using 525, 216 or 75  $k$ -points in the irreducible wedge of the Brillouin zone, respectively. The  $6s$  and  $6p$  semicore states have been treated self-consistently in a separate energy panel. In the valence panel the LMTO basis set includes functions of  $7s$ ,  $7p$ ,  $6d$  and  $5f$  character, where the  $7p$  channel has been downfolded.<sup>40</sup>

The atomic spheres approximation (ASA) is used, whereby the crystal volume is divided into slightly overlapping atom-centered spheres of a total volume equal to the actual volume. The ASA gives rise to uncontrollable errors in the evaluation of the total energy, which inhibits the comparison of energetics of different crystal structures, on account of different overlaps of the atomic spheres. In the present study the focus is on the energetics of different localization scenarios within the same crystal structure, and the ASA error is of minor influence. The spin-orbit interaction couples the band Hamiltonian for the spin-up and spin-down channels, *i.e.* a doubled

secular problem must be solved. Other relativistic effects are automatically included by solving the scalar-relativistic radial equation inside spheres. The spin-orbit parameter,

$$\xi(r) = -\frac{2}{c^2} \frac{dV}{dr},$$

in atomic Rydberg units, is calculated from the self-consistent potential.

Given the considerable disagreement between theory and experiment as to the magnetic ordering specifically in Pu and Am, we use the total energy considerations to investigate the SIC-LSD ground state with respect to both valency and spin configuration. The magnetic order is dictated by the order imposed on the localized  $f$ -states, and the paramagnetic and ferromagnetic/antiferromagnetic scenarios are implemented by considering the initial localized  $f$ -manifold to be either non-spin-polarized or spin-polarized in appropriate spatial arrangements.<sup>48</sup> During iteration to self-consistency the Wannier states may change, however roughly retaining their overall characteristics (exceptions occur close to delocalization).

Other approaches implement a non-magnetic ground state either by assumption (DMFT),<sup>24</sup> through a careful calibration of the  $U$  and  $J$  parameters in LDA+ $U$  (FLL)<sup>22</sup> or the double counting correction in LDA+ $U$  (AMF),<sup>23</sup> or by invoking disorder in the directions of local moments.<sup>19</sup>

## III. RESULTS

As described in the previous section, we consider in this work only the high symmetry crystal structures relevant for the actinide elements in their low-pressure/large specific volume phases with localized  $f$ -electrons, specifically fcc and hcp crystal structures. A few tests for the dhcp structure, which is the actual ground state structure at ambient conditions for Am, Cm and Bk, revealed virtually no difference with respect to the simpler hcp structure in terms of cohesive energy per atom, specific volume and magnetic moments. As mentioned earlier, the present ASA implementation of the SIC-LSD energy functional is not accurate enough to resolve the energy differences between these structures.

### A. Total energy considerations

In Table I, the results of our calculations are summarized. In the last column, the calculated total energy differences between the paramagnetic and magnetic configurations are shown. We find that the non-magnetic configuration is energetically most favourable for the light actinides, U and Np, while all the remaining actinides prefer the spin-polarized ground state. Thus, from SIC-LSD total energy considerations we find the calculated

TABLE I: Equilibrium volumes,  $f$ -occupation and magnetic moments of U, Np,  $\delta$ -Pu, Am, Cm, and Bk in the SIC-LSD ground state. Results for both the paramagnetic and the magnetic ground state are quoted. The numbers of localized and delocalized  $f$ -electrons are given, and for the moments both the spin and orbital moments (in Bohr magnetons,  $\mu_B$ ) are listed. All paramagnetic (PM) calculations were done for the fcc structure, while ferromagnetic (FM) calculations were performed for the fcc structure in the case of U and Np, and antiferromagnetic (AFM) calculations for the hcp structure for Pu, Am, Cm, and Bk. Last column gives the energy difference (in eV) between the paramagnetic and magnetic ground states.

	$V_0$ (a.u.)	$V_{exp}$ (a.u.)	$N_f(\text{loc})$	$N_f(\text{band})$	$M_L$	$2M_S$	$\Delta E_{PM-AFM}$ (eV)
U	140.4	138.9	0	3.07	0.0	0.0	-
Np	122.4	126.9	0	4.30	0.0	0.0	-
Pu (PM)	163.8	168	4	1.34	0.0	0.0	1.14
Pu (AFM)	207.1		5	0.35	-4.11	5.25	
Am (PM)	200.6	198	6	0.40	0.0	0.0	1.56
Am (AFM)	210.5		6	0.54	-1.59	6.45	
Cm (PM)	171.0	202	6	1.51	0	0	2.29
Cm (AFM)	203.8		7	0.26	-0.15	6.79	
Bk (PM)	205.1	189	8	0.67	0	0	1.86
Bk (AFM)	197.4		8	0.43	3.21	5.36	

ground states in agreement with experiment for U, Np, Cm, and Bk, but fail to reproduce the experimentally observed non-magnetic ground states of both Pu and Am.

The fact that total energy considerations in LSD and also SIC-LSD favour the magnetic ground state in the actinide elements Pu and Am is a manifestation of the Hund's first rule rather than a consequence of interatomic exchange being significant. Neither LSD nor SIC-LSD can describe the appropriate multi-determinant eigenstates of  $L$  and  $S$ . This leads to an error in the energy associated with local paramagnetic moments, since the exchange potential generated by the localized states and exerted on the non- $f$  electrons is determined by  $M_S$  ( $\sim S$ ). This is most clearly demonstrated for  $f^6$ , where the correct ground state according to the Hund's rules in Russell-Saunders coupling is  ${}^7F_0$ , i.e.  $S = L = 3$ ,  $J = 0$ . Hence, also  $M_S = 0$ , and accordingly no spin-dependent exchange-field is exerted on the conduction electrons by an actinide ion in the  $f^6({}^7F_0)$  configuration. But LSD sets up a large spin-dependent potential, since it can only represent the  ${}^7F_0$  ground state by  $M_S = 3$ . This description can be valid if the inter-atomic exchange interaction is strong enough for an ordered magnetic phase to be formed. However, it is an incorrect description of the cohesion of the conduction states, if the exchange interaction is not strong enough compared to the spin-orbit interaction which selects the  $J = 0$  ground state multiplet. The latter scenario occurs for Am. This also explains why the disordered local moment approach describes the actinides so well,<sup>19</sup> since the disorder (in the direction of spin quantization axis) leads to averaging of the spin-dependent part of the potential to zero.

## B. Uranium and Neptunium

Studies of the electronic structure of U and Np, have demonstrated that the observed volumes and crystal structure can be explained by the conventional band

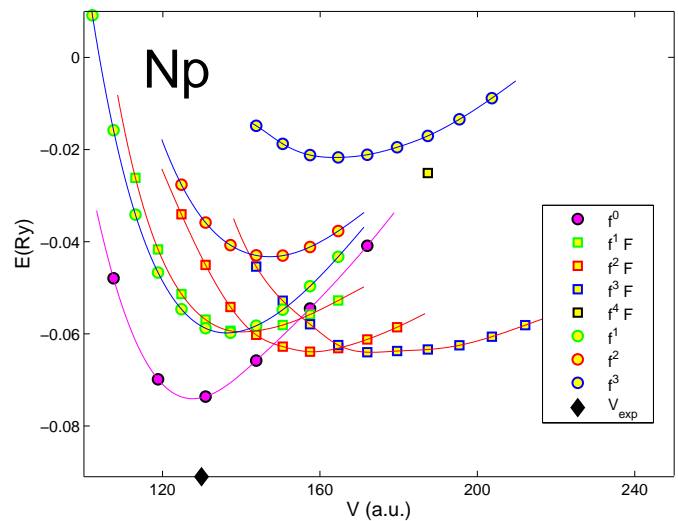


FIG. 1: (Color online) Total energy of fcc Np as function of volume for several scenarios distinguished by the different number of localized  $f$ -electrons on Np ions. Both non-magnetic (spheres) and ferromagnetic (squares) configurations are considered.

structure calculations (see for example Ref. 13 and references therein). Nevertheless, despite this overall rather good agreement with experiment there are still discussions as to what band structure approach is best suited to describe volume trends.<sup>13,49,50</sup> Furthermore, a comparison between XPS data and a fully relativistic calculation has shown that correlations already have a measurable influence on the electronic structure of Np.<sup>51</sup>

In our calculations, we compare the band- $f$  scenario, where all  $f$  electrons are treated as itinerant, to a number of localized/delocalized  $f$ -electron scenarios, and find it to be energetically most favourable for both U and Np. In figure 1, the total energy versus volume is plotted for



a number of Np  $f$ -electron configurations, both for the non-magnetic and the magnetic states. The global total energy minimum is obtained for the  $f^0$  configuration. Spin polarization is not energetically favourable, resulting in a non-magnetic ground state in agreement with experimental data for both U and Np. This indicates that correlations are relatively weak in these elements, and confirms the adequacy of the LSD picture for treating the electronic structure of the early actinides. Comparing the calculated equilibrium volumes to the experimental values, we find very good agreement for both U and Np, but with some slight overbinding in Np, as is also observed in other band structure calculations. A comparison of the difference in total energies between the LSD ground state configuration and the nearest localized configuration gives respectively 0.38 eV for U and 0.20 eV for Np, implying that the localized configuration is less unfavourable for Np, which indicates the increasing influence of correlations.

### C. Plutonium

From the theory point of view, Pu is without doubt the most interesting element of the actinide series, as witnessed by the considerable number of papers already published on the subject. Its complex phase diagram, behaviour under pressure, and the absence of magnetism have still not been fully understood to date. Within DFT a number of theoretical studies have concentrated on the magnetic ground state, where spin-polarization mimics the effect of  $f$ -electron localization, which leads to calculated lattice parameters that are in rather good agreement with the experimental values, for both the  $\alpha$ - and  $\delta$ -phase.<sup>17,21,52</sup> Other calculations have tried to take the experimentally observed non-magnetic ground state into account, either by assuming it as a starting point of their calculation<sup>19,24</sup> or by implementing it into their model by means of an adequate choice of parameters.<sup>20,22,23</sup> Using the latter approach, LDA+ $U$  calculations<sup>22,23</sup> find a non-magnetic ground state for metallic Pu in both phases, driven by a strong spin-orbit coupling in the  $5f$ -shell.

In our calculations for Pu we merge elements of both of these approaches, as in what follows we assume a non-magnetic ground state, and compare to our previously published ferromagnetic calculations.<sup>31</sup> In figure 2, the total energy of Pu in the fcc phase is displayed for several localized paramagnetic  $f^n$  configurations. Remarkably, the energy minima for the scenarios with 0, 1, 2, 3 or 4 localized states are nearly degenerate (within 0.03 eV/atom), while localizing 5  $f$ -electrons is marginally less favorable (0.11 eV/atom higher energy than the  $f^4$  scenario) and localizing 6  $f$ -electrons is 0.90 eV/atom higher in energy. The implication is that fcc Pu is situated virtually at the localization-delocalization transition at ambient pressure. The Pu  $f$ -manifold is dynamical, as the  $f$ -electrons may freely fluctuate between a localized  $f^4$  shell and a fully itinerant state. It signals an elec-

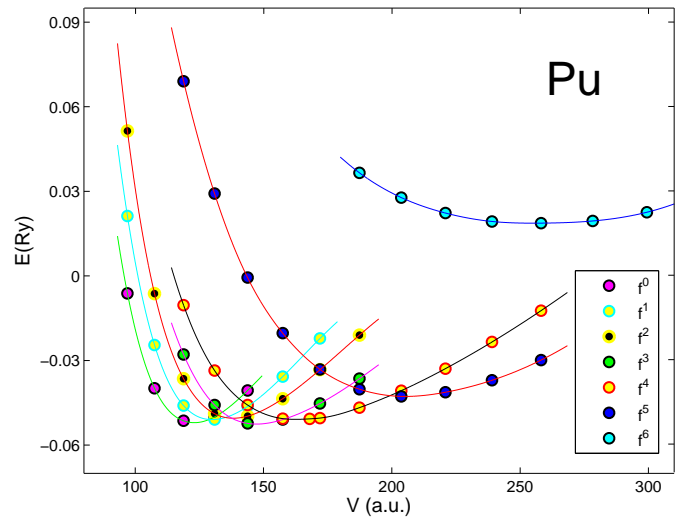


FIG. 2: (Color online) Total energy of paramagnetic fcc Pu as function of volume for several scenarios distinguished by the different number of localized  $f$ -electrons on Pu ions.

tronic wavefunction of much more complex nature than can be realized with the SIC-LSD approach, which in the usual spirit of DFT seeks to describe the many-electron system with a single Slater determinant. The equilibrium volume of the  $f^4$  state is calculated as 163.8 a.u., which is close to the experimental value for the  $\delta$ -Pu volume of 168 a.u., while the calculated equilibrium volume of the  $f^0$  state, 123.0 a.u., is close to, but smaller than, the experimental equilibrium volume of  $\alpha$ -Pu, 135 a.u., quite a typical overbinding for the LSD approximation. Hence, it is suggestive that the  $f^4$  phase be stabilized by high temperature or alloying<sup>53</sup> to form the  $\delta$ -phase of Pu, while the low symmetry crystal structure of the  $\alpha$ -phase most probably stabilizes the  $f^0$  scenario.

In figure 3 the density of states (DOS) of a number of these localization scenarios is displayed. In the LSD scenario of figure 3a, the  $f$ -manifold is split into a  $j = 5/2$  and a  $j = 7/2$  band by the spin-orbit interaction. The exchange interaction is absent here, and the additional splitting within each of the two groups of bands is due to crystal field effects. Here the Fermi level is situated at the top of the filled  $j = 5/2$  band, with a resulting large DOS at the Fermi level. In Fig. 3b, which represent the DOS of the  $f^4$  paramagnetic configuration, four of the  $f$ -states treated as band states in Fig. 3a, have become localized, leaving the remaining  $f$ -states available for band-formation. The width of the valence bands is 5 eV, however with most of the weight in the region from the Fermi level to 2.5 eV below the Fermi energy. A considerable hybridization of band  $f$ -states is seen in the range from -1 eV below to the Fermi level, including a high density of states at the Fermi level, in agreement with the experimental photoemission spectrum<sup>7</sup> and the high specific heat<sup>54</sup> of  $\delta$ -Pu. We note however that a

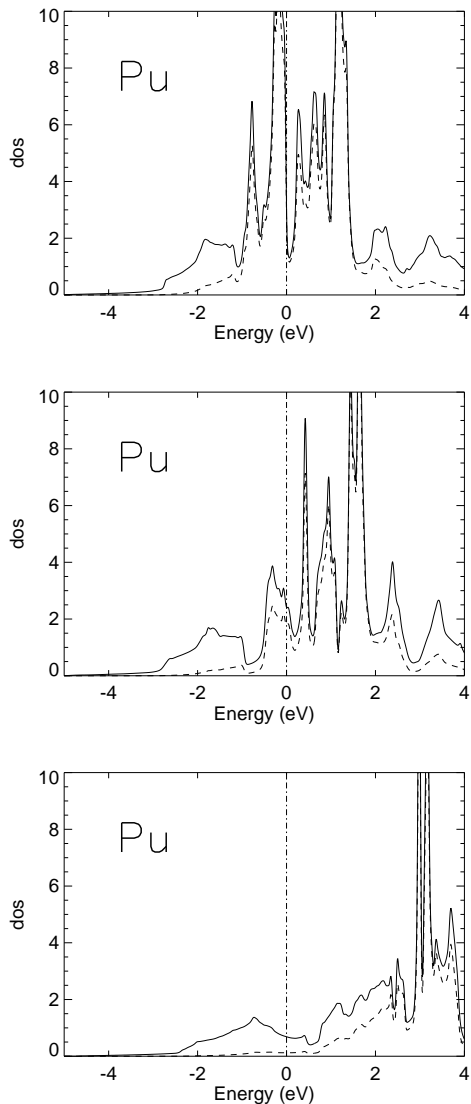


FIG. 3: Density of states of paramagnetic fcc plutonium in a) the LSD scenario b) the localized  $f^4$  scenario and c) the localized  $f^6$  scenario. Full line is the total density of states, while dashed line gives the  $f$  partial density of states. Units are states per atom and per eV, and the energy is given relative to the Fermi level.

photoemission spectrum is not directly comparable to a theoretical density of states, which strictly speaking only provides information on how the ground state is constructed from one-particle states, while the final excited states play a crucial role in the photoemission spectrum.

In the earlier SIC-LSD calculation<sup>31</sup>, assuming a ferromagnetic ordering, we found a Pu ground state comprised of localized  $f^5$  ions, with much too large a volume (30 % overestimate), quite like the paramagnetic  $f^5$  scenario in figure 2, which has a minimum volume around 205 a.u.. By invoking ferromagnetic order in the LDA+U (FLL)

calculations, Refs. 20,21,23 also concluded on an  $f^5$  localized ground state. The recent LDA+U calculations of Ref. 22 based on a reduced exchange interaction determined a non-magnetic ground state characterized by  $f^6$  ions, with a vanishing DOS at the Fermi level. A similar picture emerges from our SIC-LSD DOS for the  $f^6$  configuration, shown in Fig. 3c. Energetically we find this configuration unfavourable by almost 1 eV, and the absence of any noticeable DOS at the Fermi level is in disagreement with experiment. The AMF flavour of LDA+U finds  $\delta$ -Pu in a mixed valent state<sup>23</sup> with a total  $f$ -occupancy of 5.44. In a recent DMFT calculation,<sup>55</sup> Pu is similarly described as being in a mixed valence state (strong peak around the  $f^5$  configuration), with an average  $f$ -occupancy of 5.2, while another DMFT calculation using a different impurity solver suggest a value around 5.8.<sup>34</sup> The integrated number of band  $f$ -states in our  $f^4$  configuration is 1.34, therefore the total number of  $f$ -electrons in  $\delta$ -Pu comes out to be 5.34 (see Table I). This result is markedly different from the situation in the rare earths where the number of delocalized  $f$ -electrons never exceeds about 0.7,<sup>45</sup> *i. e.* significantly more  $f$ -electrons are involved in the cohesion in  $\delta$ -Pu at ambient conditions. The total number of  $f$ -electrons is nearly a constant in the various localization scenarios  $f^0$  -  $f^5$  ( $N_f = 5.48, 5.42, 5.36, 5.36, 5.34, 5.39$ , respectively), *i. e.* what distinguishes these cases is the ratio of localized to delocalized  $f$ -electrons. The  $f^6$  scenario becomes energetically unfavorable (figure 2) precisely because it forces a high  $f$ -occupancy on Pu ( $N_f = 5.93$ , slightly below 6 due to the tails of localized states reaching into the neighbouring sites), which involves a relatively high intraatomic Coulomb interaction energy.

The localized  $f$ -states are not shown in figure 3, since their SIC band energies are poor estimates of physical removal energies. A rough estimate of removal energies of the localized states may be obtained by the transition state argument,<sup>56</sup> which when applied to the  $f^4$  state of Pu places the localized states at -3.1 eV. In experiments,<sup>7</sup> there is no evidence of particularly strong emission at this energy, so this aspect of the electronic structure of  $\delta$ -Pu remains a puzzle.

In conclusion, it emerges that the paramagnetic SIC-LSD implementation describes the fcc phase of Pu satisfactorily, while the combination of the self-interaction correction and the exchange energy in the magnetic limit overestimates the tendency to localization. Experimentally, the vanishing of magnetic moments in Pu was recently re-confirmed.<sup>10</sup> Furthermore, electron energy loss spectroscopy branching ratios<sup>12,47</sup> clearly favor the  $jj$ -coupling picture over the  $LS$ -coupling (for  $\alpha$ -Pu).

#### D. Americium

The SIC-LSD total energy curves for americium are displayed in figure 4. As for Pu we have investigated several localization scenarios from  $f^0$  to  $f^7$ , assuming a para-

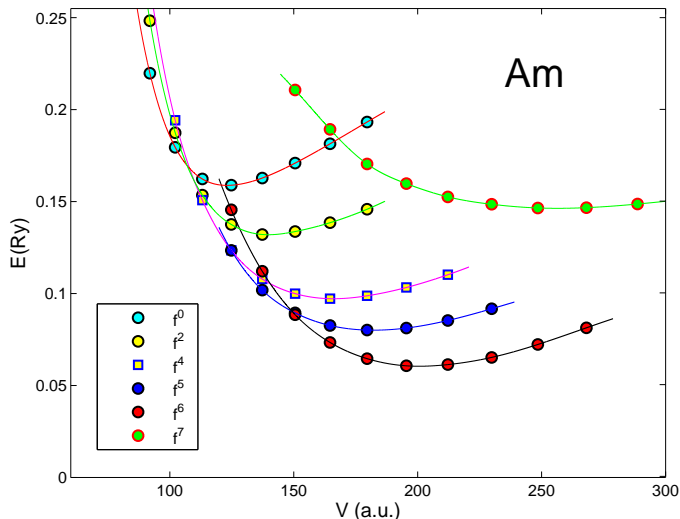


FIG. 4: (Color online) Total energy of paramagnetic fcc Am as function of volume. Several paramagnetic configurations of the localized  $5f$  subshell are considered, as discussed in text.

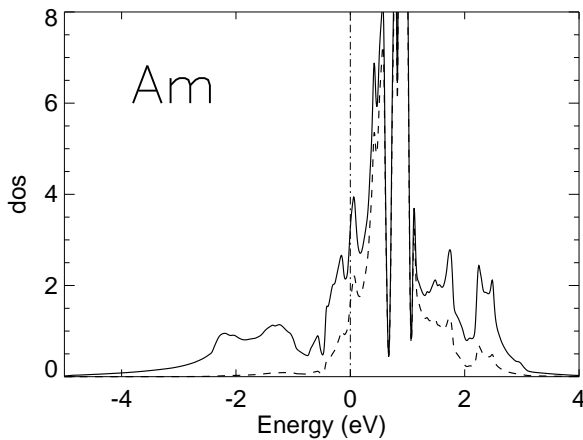


FIG. 5: Density of states of hcp americium in the paramagnetic state with 6 localized  $f$ -electrons per Am atom at  $V = V_0 = 200.6$  a.u.. Full line is the total density of states, while dashed line gives the  $f$  partial density of states. Units are as in figure 3. Only the itinerant electron states are shown. The localized states by the transition state argument may be estimated to be situated around  $-4.0$  eV.

magnetic phase. The lowest energy is found for the  $f^6$  configuration with an equilibrium volume of  $V_0 = 200.6$  a.u. per atom, which matches perfectly with the experimental volume of  $V_{exp} = 198$  a.u.. At this volume the  $f^5$  configuration is  $0.27$  eV higher, and the  $f^7$  configuration is  $1.4$  eV higher, i.e. the  $f^6$  ground state appears quite robust at ambient conditions, contrary to the situation in Pu. This result is in agreement with recent photoemission studies<sup>57</sup> that measure a solid  $f^6$  ground state

configuration. A non-magnetic  $f^6$  ground state configuration has also been suggested on the basis of LDA+ $U$  (AMF) calculations.<sup>32</sup>

The density of band states of Am in the paramagnetic  $f^6$  ground state is displayed in Fig. 5. The calculation shown has been performed for the hcp closed packed structure, but the density of states of the fcc structure is very similar. The Am  $f$ -bands are almost exclusively of  $j = 7/2$  character and situated around  $1$  eV above the Fermi level, with a small tail extending below the Fermi level. The total number of  $f$ -electrons is  $N_f = 6.40$ , i.e. approximately  $0.4$   $f$ -electrons reside in this tail. The localized states are not shown in the figure but the transition state estimate places them at an energy  $\sim -4.0$  eV. Compared to  $\delta$ -Pu, Am has approximately one less band  $f$  electron, slightly deeper localized states and more narrow unoccupied  $f$ -bands. Early photoemission experiments<sup>58</sup> on Am reveal the localized states as a plateau between  $2$  and  $4$  eV below the Fermi level, with traces of  $f^7$  character<sup>27,59</sup> between  $-2$  and  $-1$  eV, however with virtually no  $f$ -related emission at the Fermi level. Hence the electronic structure of Am is very different from that of  $\delta$ -Pu. The photoemission spectra have been interpreted in terms of a mixed valent ground state of fluctuating  $f^6$  and  $f^7$  configurations,<sup>27</sup> dominated by the former. The present SIC-LSD ground state, comprised of firm  $f^6$  ions coexisting with a tail of  $0.4$  band  $f$  electrons, can be considered a reasonable representation of the same mixed valent ground state.

Upon compression the Am  $f$ -shell becomes more and more active in the bonding, as illustrated in figure 4, where the energy curves of the configurations with fewer localized/more delocalized  $f$ -electrons come closer to the  $f^6$  curve. At a compression around  $V/V_0 = 0.75$  the  $f^5$  curve becomes lower in energy, around  $V/V_0 = 0.65$  the  $f^4$  curve dips below and becomes most favorable and so on, until around  $V/V_0 = 0.52$  eventually the  $f^0$  curve becomes the lowest, meaning that the lowest energy is obtained with complete band-description of the  $f$ -electrons. Hence the  $f$ -delocalization happens gradually in the volume range between  $V/V_0 \equiv 0.75$  and  $V/V_0 \equiv 0.52$ . In terms of pressure, this corresponds to the range  $p = 16$  GPa to  $p = 35$  GPa, as given by the common tangents of the respective energy curves. Of course, since the crystal structure in figure 4 is fixed to be fcc this is not directly comparable to the experimental behavior of Am under pressure,<sup>60</sup> where the  $f$ -electron delocalization is accompanied by a sequence of structural changes. However, if we assume that the AmI (dhcp) and AmII (fcc) phases are indicative of localized  $f$ -electrons, the experimental onset of delocalization is at the AmII–AmIII phase transition, which occurs at  $V/V_0 = 0.77$  and  $p = 10.0$  GPa. The  $f$ -electron delocalization is presumably nearly complete in the AmIV (primitive orthorhombic), which is obtained at  $V/V_0 = 0.63$  and  $p = 17.5$  GPa. This volume is larger than the  $V/V_0 = 0.52$  deduced from theory, most probably due to the different crystal structure, as it is well known that  $f$ -electron delocalization favors

lower symmetry lattices<sup>61</sup> and vice versa. The interpretation of the AmIII (face centered orthorhombic) as a structure of intermediate  $f$ -electron delocalization is also corroborated by total energy calculations,<sup>18</sup> for which additional  $f$ -correlations (in the form of anti-ferromagnetic spin-polarization and orbital polarization) need to be incorporated to achieve accurate description. Hence, there is qualitative agreement between the SIC-LSD theory of  $f$  electron delocalization under pressure and experimental observations for americium.

In our earlier SIC-LSD study of americium<sup>31</sup> only the ferromagnetic spin arrangement was considered. The calculated ground state configuration was also  $f^6$ , however with an 8 % too large equilibrium volume, and the  $f^7$  configuration only 0.12 eV higher in energy. In addition, the spin and orbital moments were far from cancelling ( $M_S = 3.41\mu_B$ ,  $M_L = -1.58\mu_B$ , where  $\mu_B$  is a Bohr magneton). The situation is slightly improved by allowing for an antiferromagnetic spin arrangement. In the hcp structure, the energy per atom is lowered by 0.03 eV in the antiferromagnetic structure compared to the ferromagnetic arrangement, and the equilibrium volume is lowered by 5 %, but the moments remain almost unchanged ( $M_S = 3.23\mu_B$ ,  $M_L = -1.59\mu_B$ ). Hence, antiferromagnetic ordering constitutes the lowest energy solution of the SIC-LSD minimization. Overall, however, the paramagnetic scenario provides the best description of the elemental americium, while imposing an antiferromagnetic order can only be considered as a simple means of partially patching up the bonding properties. A SIC-LSD study on Am pnictides and chalcogenides predicted large DOS at the Fermi level, in agreement with susceptibility measurements<sup>62</sup>, but not observed in photoemission studies.<sup>57</sup> The results were obtained based on the assumption of a magnetic ordering, but invoking instead a paramagnetic state might provide some new insight into their electronic structure.

### E. Curium

The SIC-LSD total energy of curium is shown for both the magnetic and paramagnetic scenarios in figure 6. For simplicity, only the fcc structure is considered, except for a few calculations performed with antiferromagnetic spin arrangement in the hcp structure (asterisks in figure 6). The half-filled  $f^7$  configuration of localized states is seen to give the minimum, at a volume of  $V = 203.8$  a.u., which is in good agreement with the experimental equilibrium volume. From Table I, and figure 6, we find the paramagnetic scenario unfavourable in energy with respect to the anti-ferromagnetic scenario by 2.3 eV. Here the magnetic state with localized  $f^7$  ions having  $S = 7/2$ ,  $L = 0$ , and  $J = 7/2$ , provides an adequate description of Cm. The paramagnetic state in this case gives a poorer description, with  $f^6$  localized  $f$  shells and a 17 % too small volume. The antiferromagnetic state is lower than the ferromagnetic by 0.04 eV per atom in the

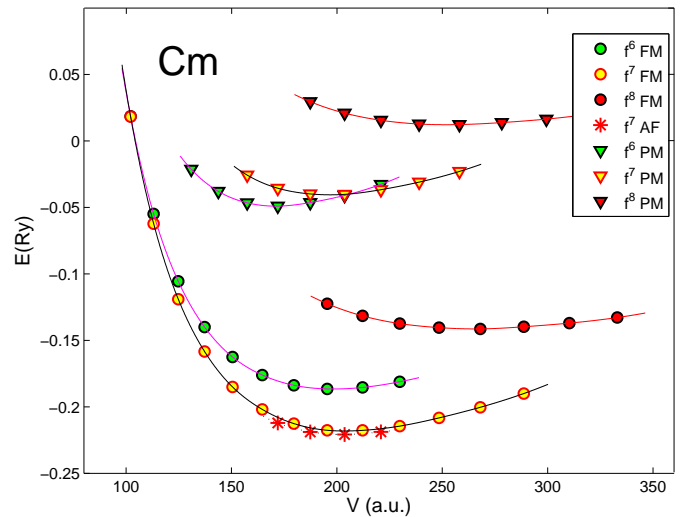


FIG. 6: (Color online) Total energy of fcc Cm as function of volume for several scenarios differing with respect to the number of localized  $f$ -electrons on Cm, notably 6, 7, or 8 localized  $f$ -electrons. The balls correspond to the ferromagnetic ordering scenario, while triangles correspond to the non-magnetic scenario, as discussed in text. In addition, the asterisks correspond to hcp antiferromagnetic arrangement of  $f^7$  curium atoms.

hcp structure, but we are not able to resolve the structural energy difference between the very similar fcc, hcp and dhcp phases. The antiferromagnetic phase is also observed experimentally.<sup>63</sup> A recent DMFT<sup>55</sup> study has similarly established the  $f^7$  atomic configuration for Cm.

The relative stability of the half-filled  $f^7$  shell is evidenced by the high compression ( $V/V_0 \sim 0.60$ ) needed for the next delocalization step,  $f^6$ , to be of comparable energy. This is also in accord with the higher pressure needed experimentally to convert Cm into a low symmetry structure indicative of  $f$ -contribution to bonding (CmIII monoclinic structure), appearing at  $p = 37$  GPa and  $V/V_0 = 0.65$ .<sup>11</sup>

### F. Berkelium

The SIC-LSD total energies as a function of volume, calculated for berkelium in the fcc structure and the ferromagnetic spin-alignment, are shown in figure 7. The localization  $f^n$  scenarios, with  $n = 0, 1, \dots, 8$ , have been considered, for both magnetic and paramagnetic states, but only the magnetic configurations are shown in the figure. The ground state is found for an  $f^8$  localized shell, at a volume  $V = 201.4$  a.u., which is 6 % larger than the experimental equilibrium volume. The energy difference between the ferromagnetic and antiferromagnetic arrangements in the hcp structure is quite small,  $\sim 0.02$  eV per atom, in favor of the latter. The equilibrium volume at the same time decreases to 197.4 a.u., which is a



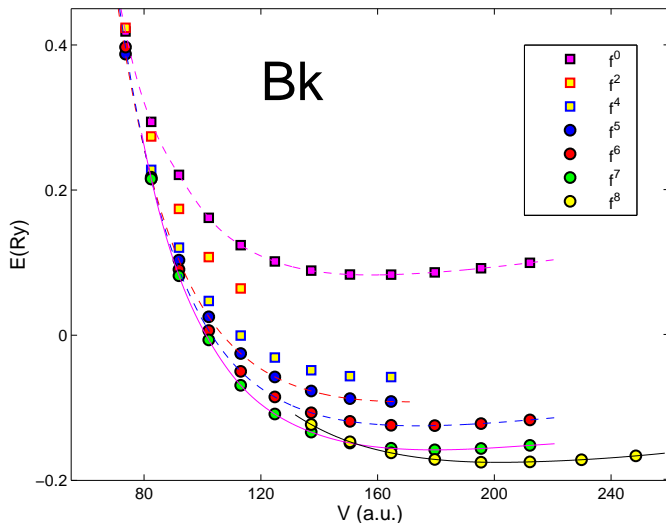


FIG. 7: (Color online) Total energy of ferromagnetic fcc Bk as function of volume for several scenarios differing with respect to the number of localized  $f$ -electrons on Bk.

small improvement over the ferromagnetic volume. The number of band  $f$ -electrons is 0.43. The magnetic moments of the Bk atom are large,  $M_L = 3.21\mu_B$ ,  $2M_S = 5.36\mu_B$ , leading to a total moment of  $M = 8.57\mu_B$ . The experimental moment of Bk is even higher,  $\mu_{\text{eff}} = 9.8\mu_B$  (Ref. 63), leading to a projected value  $M \sim 9.05$ , i.e. very close to that of a pure  $f^8$  Hund's rule coupled ion (here we assumed a  $g$ -factor of 1.5 as appropriate for  $f^8$ ).

The configuration with an  $f^7$  localized shell is 0.23 eV higher in energy. This state has 1.45 band-like  $f$ -electrons. Upon compression this scenario becomes progressively more important, and at  $V/V_0 = 0.75$  it becomes lower in energy. The high stability of the  $f^7$  shell is manifested through this remaining the lowest energy scenario up to compressions of  $V/V_0 = 0.40$ , after which the  $f$  manifold quickly delocalizes. The transition pressure, corresponding to the common tangent between the  $f^8$  and  $f^7$  total energy curves, is  $p = 15$  GPa. Experimentally, Bk is observed in the dhcp phase under pressures up to  $p = 7-8$  GPa, after which the fcc phase occurs and is stable up to  $p = 25$  GPa and  $V/V_0 = 0.70$ .<sup>64</sup> At pressures above 25 GPa a low symmetry phase, possibly of  $\alpha$ -U type, is observed. The conventional interpretation<sup>4</sup> is that the first two highly symmetric crystal structures are associated with localized  $f$ -electrons, and hence that  $f$ -delocalization sets in at 25 GPa, which is somewhat higher than the theoretical value found here, but acceptable within our limits of accuracy. It would be interesting to investigate whether signatures of a state characterized by  $f$ -electrons in a mixed  $f^7$  localized and 1.5  $f$  itinerant picture could be observed for berkelium. Such a state would have similarity to the  $\delta$ -Pu phase, i.e. both distinct localized features, like deep-lying  $f$ -states in photoemission, and itinerant characteristics, like a large density of

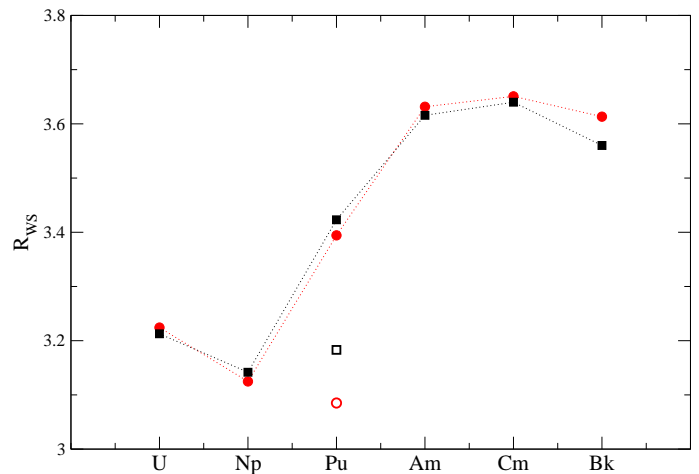


FIG. 8: (Color online) Trends in the Wigner-Seitz radius through the actinide series. The (red) circles and (black) squares are calculated (in fcc structure) and experimental Wigner-Seitz radii, respectively. For Pu the  $f^4$  non-magnetic ground state is taken and compared with the experimental Wigner-Seitz radius of  $\delta$ -Pu. The calculated ( $f^0$ ) and experimental  $\alpha$ -Pu Wigner-Seitz radii are marked with an open circle and an open square, respectively.

states at the Fermi level. However, in contrast to  $\delta$ -Pu the Bk atoms would possess large magnetic moments, arranged antiferromagnetically. The present study is restricted to the high-symmetry structures fcc, hcp and dhcp, and thus it cannot be excluded that around the  $f$ -delocalization transition the energy gain by full delocalization and adoption of an appropriate low-symmetry phase outweighs that of only partial delocalization.

The paramagnetic scenario was also investigated for Bk (not shown). Energetically, this state is unfavorable (see Table I), but also other aspects of the calculation are in disagreement with experiment. The  $f^8$  localized shell is found to be the lowest energy state in this case, with an equilibrium volume of  $V = 205.1$  a.u., i.e. somewhat larger than the volume of the magnetic phase. However the  $f^7$  localized scenario is very close in energy (0.02 eV per atom), implying a possible low-pressure ( $p \sim 1$  GPa) transition to this state, which furthermore would be accompanied by a  $\sim 10\%$  volume discontinuity. Experimentally, there is clear evidence of large antiferromagnetically ordered moments.<sup>63</sup>

#### IV. DISCUSSION

Table I and figures 8, 9, and 10 summarize the findings of the present paper. The rather good agreement between calculated and experimental Wigner-Seitz radii is demonstrated in Fig. 8. Figure 9 shows the calculated number of band-like  $f$ -electrons in the ground state. It is seen to rise steeply from U to  $\alpha$ -Pu, reflecting the filling of the  $f$ -band, before dropping dramatically towards the

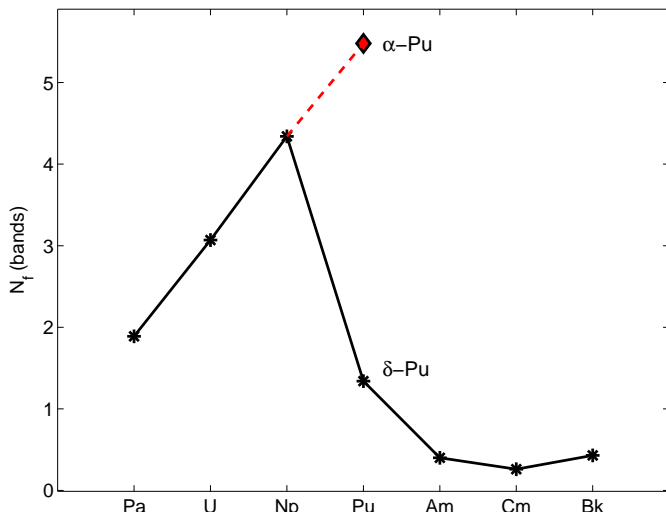


FIG. 9: Trends in the the number of band  $f$  electrons through the actinide series. For Pu, the  $\alpha$ - and  $\delta$ -phases are identified with the  $f^0$  and  $f^4$  paramagnetic states, respectively.

heavier actinides, reaching its lowest value for Cm, after which a small increase is seen again for Bk. For  $\delta$ -Pu, an intermediate  $f$ -band filling is found, which elucidates the extraordinary character of this element, also clear from the essentially vanishing localization/delocalization energy illustrated in figure 2. Correlating Fig. 8 to Fig. 9, it follows that the increasing number of band-like  $f$  electrons for U, Np and Pu( $f^0$ ) contributes to the bonding and leads to the observed smaller equilibrium volumes, while larger volumes are obtained for Am, Cm, and Bk, having a few band-like  $f$  electrons.

Several important energy scales may be identified for the actinide elements. The intraatomic exchange field is undoubtedly relevant but cannot be comprehensively addressed by the single-determinant description underlying the DFT, by which the atomic  $S$  and  $M_S$  quantum numbers get mixed up. In our calculations this shortcoming translates into wrong predictions of magnetic ground state configurations of Pu and Am. The energy scale for the interatomic exchange interaction is small, favoring the antiferromagnetic arrangement over the ferromagnetic arrangement with 0.02-0.04 eV per atom in Pu, Am, Cm and Bk. The localization/delocalization energy scale is larger but depends strongly on volume.<sup>31</sup> As a consequence,  $f$ -electrons are eventually transferred from being localized to becoming band-like when pressure is applied. In figure 10, we show the trends in the range of relative volume over which the  $f$ -electron delocalization takes place for Pu to Bk. The volume range where the  $f$ -electron delocalization occurs is defined in theory by the lowest volume having the same number of localized electrons as in the ground state (onset), and the largest volume where a completely delocalized ( $f^0$ )  $f$ -manifold occurs. In experiment there is no clear-cut definition, but

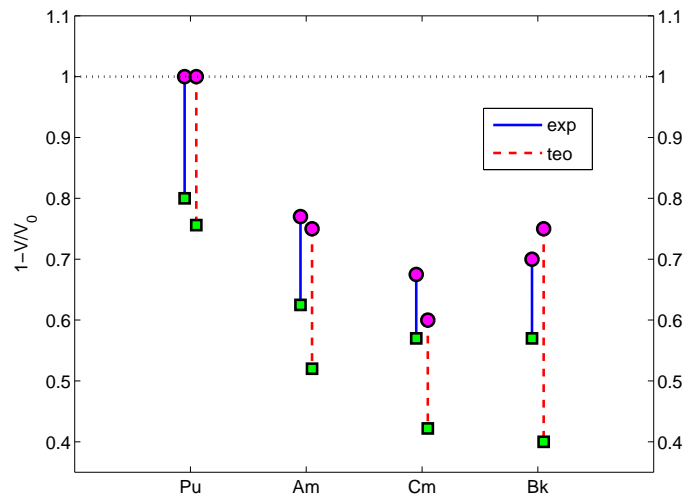


FIG. 10: (Color online) Trends in the ranges of volumes of  $f$  electron delocalization in the actinide elements. Onset (completion) of delocalization is marked with balls (squares), for each element with experimental data (blue and full line) to the left and theoretical data (red and dashed line) to the right. Volumes are given relative to the (localized) equilibrium volume at ambient conditions. Experimental ranges are defined by the smallest volumes observed in the high-symmetry (fcc) phase and the largest volumes observed for the low-symmetry ( $\alpha$ -U type or similar) phases in high pressure experiments (Refs. 60, 11, 64; for Pu the range is defined by the zero pressure volumes of the  $\delta$ - and  $\alpha$ -phases). The theoretical ranges are defined within the fcc structure only.

presumably as long as the crystal phase remains fcc under compression, the  $f$ -shell is completely localized, whereas a complete delocalization may be assumed to have occurred once the high-pressure low-symmetry phases of AmIV,<sup>60</sup> CmIV,<sup>11</sup> and BkIII<sup>64</sup> are reached. The trends of experiments and theory are in agreement, with Pu at the delocalization threshold under ambient conditions, and Cm the most stable of the actinide elements studied. The theoretical volumes of  $f$  delocalization completion tend to be smaller than the experimental ones, which most probably is due to the restriction of the present calculations to the high-symmetry fcc and hexagonal phases.

A striking result of the calculations presented here is that an excellent account of the cohesive properties of the localized phases of the actinide elements can only be achieved, if  $\delta$ -Pu and Am are described by a paramagnetic phase, while a magnetic phase is appropriate for Cm and Bk. The SIC-LSD total energy functional incorrectly favors the formation of a magnetic state for  $\delta$ -Pu and Am. The reason for this shortcoming is probably different for these two elements. In Pu, the  $f$ -shell is in a vividly fluctuating state, and presumably any tendency to form interatomic magnetic correlations is washed away by quantum fluctuations. In Am, the  $f^6$  shell is more robust against fluctuations, but here the overestimated tendency to form a magnetic state can be traced back to

the inadequacy of the LSD to describe Russell-Saunders coupling and the formation of Hund's rules ground states, as discussed in section III.A.

Due to its construction, the SIC-LSD can only describe an integer number of localized states on each atom, and the delocalization process upon compression is modelled as a series of steps, characterized by one more  $f$ -electron changing from atomic to band-like behavior. Such a description can only be considered approximative, and in a more elaborate theory the transitions are likely to occur continuously. To describe these continuous transitions at finite temperature we can construct a mean-field coherent potential approximation of the fluctuating localization configurations distinguished by different numbers of localized states. This has already been implemented for cerium,<sup>65</sup> and a similar study for the actinides is in progress. Bk may be an exception, due to the high stability of the  $f^7$  shell, and one may envisage a pressure range where the  $f^7$  shell is still localized while the eighth  $f$  electron, of spin minority character, has delocalized. This would be an interesting effect to look for. A more complete study of the delocalization process would also need to consider the effects of crystal structure, as it is well known that  $f$ -electrons once starting to form bands also prefer low-symmetry structures. This necessitates a full-potential description of the total energy, which will be subject of future development of the SIC-LSD method.

Finally, the most important point of Fig.10, namely Pu situated at the delocalisation threshold under ambient conditions, and trivalent Cm to be the most stable actinide studied here, is confirmed by a recent DMFT calculation.<sup>55</sup> This SIC-LSD result shows that the SIC approach is capable of identifying the important valence states across which the DMFT has to fluctuate dynamically: more or less all possible valence fluctuations for Pu, and the pure trivalent state for Cm.

## V. SUMMARY

The cohesive and electronic properties of the actinide elements U, Np, Pu, Am, Cm and Bk have been investigated with the self-interaction corrected local spin density approximations. The predicted non-

magnetic/magnetic ground states are in agreement with experiment for the light actinides U, and Np, and the later actinides Cm and Bk, but a magnetic ground state is wrongly predicted for Am and Pu. However, an accurate description has been obtained (see Table I), when Pu and Am are forced into a paramagnetic state. Cm and Bk are correctly described in an antiferromagnetic arrangement. U and Np prefer a non-magnetic delocalized  $f$  ground state configuration. The ground states at zero temperature and pressure are the trivalent Am( $f^6$ ), Cm( $f^7$ ), and Bk( $f^8$ ), while Pu shows almost degeneracy between any of the localization configurations from  $f^0$  to  $f^4$ . The latter signals a true ground state of a much more complex nature than can be described with the present approach, characterized by quantum fluctuations between any of these states. If the stabilization of Pu( $f^4$ ) with high temperature or Ga alloying is envisaged, this state may be identified with the  $\delta$ -phase of Pu, with an intermediate number of localized and itinerant  $f$ -electrons and an accompanying large density of states at the Fermi level. The delocalization of the  $f$ -shell under compression has been studied, and the delocalization has been found to occur over a range of volumes, with the established trends in good agreement with experiments. However, to describe the actual high pressure crystal structures and the structural transitions, a more accurate implementation of SIC-LSD, most notably including full non-spherical potentials, is necessary.

## VI. ACKNOWLEDGEMENTS

Discussion with B. Johansson are greatly acknowledged. This work was partially funded by the EU Research Training Network (contract:HPRN-CT-2002-00295) 'Ab-initio Computation of Electronic Properties of  $f$ -electron Materials'. AS acknowledges support from the Danish Center for Scientific Computing. Work of LP was sponsored by the Office of Basic Energy Sciences, U.S. Department of Energy. A portion of this research was conducted at the Center for Nanophase Materials Sciences, which is sponsored at Oak Ridge National Laboratory by the Division of Scientific User Facilities, U.S. Department of Energy.

---

<sup>1</sup> *The Actinides: Electronic Structure and related Properties*, ed. by A. J. Freeman and J. B. Darby, Jr. (Academic Press, New York, 1974).

<sup>2</sup> *Handbook on the Physics and Chemistry of the Actinides*, ed. by A. J. Freeman and G. H. Lander, (North-Holland, Amsterdam, 1984-87).

<sup>3</sup> B. Johansson, H. L. Skriver, and O. K. Andersen, in *Physics of Solids Under High Pressure*, ed. by J. S. Schilling and R. N. Shelton (North-Holland, Amsterdam, 1981) p. 245.

<sup>4</sup> B. Johansson, Phys. Rev. B **11**, 2740 (1975); Hyp. Int.

**128**, 41 (2000).

<sup>5</sup> S. S. Hecker, D. R. Harbur, and T. G. Zocco, Prog. Mater. Sci. **49**, 429 (2004).

<sup>6</sup> U. Benedict, in *Handbook on the Physics and Chemistry of the Actinides*, Vol. 5, edited by A. J. Freeman and G. H. Lander (North-Holland, Amsterdam, 1984-1987), chapter 3.

<sup>7</sup> A. J. Arko, J. J. Joyce, L. Morales, J. Wills, J. Lashley, F. Wastin, and J. Rebizant, Phys. Rev. B **62**, 1773 (2000).

<sup>8</sup> L. Havela, F. Wastin, J. Rebizant, and T. Gouder, Phys. Rev. B **68**, 85101 (2003).

- <sup>9</sup> T. Durakiewicz, J. J. Joyce, G. H. Lander, C. G. Olson, M. T. Butterfield, E. Guziewicz, A. J. Arko, L. Morales, J. Rebizant, K. Mattenberger, and O. Vogt, *Phys. Rev. B* **70**, 205103 (2004).
- <sup>10</sup> J. C. Lashley, A. Lawson, R. J. McQueeney, and G. H. Lander, *Phys. Rev. B* **72**, 054416 (2005).
- <sup>11</sup> S. Heathman, R. G. Haire, T. Le Bihan, A. Lindbaum, M. Idiri, P. Normile, S. Li, R. Ahuja, B. Johansson, and G. H. Lander, *Science*, **309**, 110 (2005).
- <sup>12</sup> K. T. Moore, G. van der Laan, J. G. Tobin, B. W. Chung, M. A. Wall, and A. J. Schwartz, *Ultramicroscopy*, **106**, 261 (2006).
- <sup>13</sup> M. D. Jones, J. C. Boettger, R. C. Albers, and D. J. Singh, *Phys. Rev. B* **61**, 4644 (2000).
- <sup>14</sup> M. Pénicaud, *J. Phys: Condens. Matter* **9**, 6341 (1997).
- <sup>15</sup> H. L. Skriver, O. K. Andersen, and B. Johansson, *Phys. Rev. Lett.* **41**, 42 (1978); *ibid.*, **44**, 1230 (1980).
- <sup>16</sup> P. Söderlind, *Adv. Phys.* **47**, 959 (1998); *Europhys. Lett.* **55**, 525 (2001).
- <sup>17</sup> P. Söderlind and B. Sadigh, *Phys. Rev. Lett.* **92**, 185702 (2004).
- <sup>18</sup> P. Söderlind and A. Landa, *Phys. Rev. B* **72**, 024109 (2005).
- <sup>19</sup> A. M. N. Niklasson, J. M. Wills, M. I. Katsnelson, I. A. Abrikosov, O. Eriksson, and B. Johansson, *Phys. Rev. B* **67**, 235105 (2003).
- <sup>20</sup> S. Y. Savrasov and G. Kotliar, *Phys. Rev. Lett.* **84**, 3670 (2000).
- <sup>21</sup> J. Bouchet, B. Siberchicot, F. Jollet and A. Pasturel, *J. Phys.: Condens. Matter*, **12**, 1723 (2000).
- <sup>22</sup> A. O. Shorikov, A. V. Lukoyanov, M. A. Korotin, and V. I. Anisimov, *Phys. Rev. B* **72**, 024458 (2005).
- <sup>23</sup> A. B. Shick, V. Drchal, and L. Havela, *Europhys. Lett.* **69**, 588 (2005).
- <sup>24</sup> S. Y. Savrasov, G. Kotliar, and E. Abrahams, *Nature*, **410**, 793 (2001).
- <sup>25</sup> X. Dai, S. Y. Savrasov, G. Kotliar, A. Migliori, H. Ledbetter, and E. Abrahams, *Science*, **300**, 953 (2003).
- <sup>26</sup> S. Y. Savrasov, K. Haule, and G. Kotliar, *Phys. Rev. Lett.* **96**, 036404 (2006).
- <sup>27</sup> A. Svane, *Solid State Commun.* **140**, 364 (2006).
- <sup>28</sup> M. S. S. Brooks, B. Johansson, and H. L. Skriver, in *Handbook on the Physics and Chemistry of the Actinides*, Vol. 1, edited by A. J. Freeman and G. H. Lander (North-Holland, Amsterdam, 1984-1987), chapter 3.
- <sup>29</sup> O. Eriksson, M. S. S. Brooks, and B. Johansson, *J. Less-Common Metals*, **158**, 207 (1990).
- <sup>30</sup> O. Eriksson, J. D. Becker, A. V. Balatsky, and J. M. Wills, *J. All. Comp.* **287**, 1, (1999).
- <sup>31</sup> L. Petit, A. Svane, W. M. Temmerman, and Z. Szotek, *Solid State Commun.* **116**, 379 (2000).
- <sup>32</sup> A. B. Shick, L. Havela, J. Kolorenc, V. Drchal, T. Gouder, and P. M. Oppeneer, *Phys. Rev B* **73**, 104415 (2006).
- <sup>33</sup> A. Georges, G. Kotliar, W. Krauth, and M. J. Rozenberg, *Rev. Mod. Phys.* **68**, 13 (1996).
- <sup>34</sup> L. V. Pourovskii, M. I. Katsnelson, A. I. Lichtenstein, L. Havela, T. Gouder, F. Wastin, A. B. Shick, V. Drchal, and G. H. Lander, *Europhys. Lett.* **74**, 479 (2006).
- <sup>35</sup> S. Biermann, F. Aryasetiawan, and A. Georges, *Phys. Rev. Lett.* **90**, 86402 (2003); F. Aryasetiawan, M. Imada, A. Georges, G. Kotliar, S. Biermann, and A. I. Lichtenstein, *Phys. Rev. B* **70**, 195104 (2004).
- <sup>36</sup> J. P. Perdew and A. Zunger, *Phys. Rev. B* **23**, 5048 (1981).
- <sup>37</sup> W. M. Temmerman, A. Svane, Z. Szotek and H. Winter, in *Electronic Density Functional Theory: Recent Progress and New Directions*, Eds. J. F. Dobson, G. Vignale and M. P. Das (Plenum, NY 1998.), p. 327.
- <sup>38</sup> A. Svane, *Phys. Rev. B* **53**, 4275 (1996).
- <sup>39</sup> A. Svane, W. M. Temmerman, Z. Szotek, J. Lægsgaard, and H. Winter, *Int. J. Quantum Chem.* **77**, 799 (2000).
- <sup>40</sup> O. K. Andersen, *Phys. Rev. B* **12**, 3060 (1975); O. K. Andersen and O. Jepsen, *Phys. Rev. Lett.* **53**, 2571 (1984).
- <sup>41</sup> A. Svane, P. Strange, W. M. Temmerman, Z. Szotek, H. Winter, and L. Petit, *phys. stat. sol. (b)* **223**, 105 (2001).
- <sup>42</sup> L. Petit, A. Svane, Z. Szotek, P. Strange, H. Winter, and W. M. Temmerman, *J. Phys.: Condens. Matter* **13**, 8697 (2001).
- <sup>43</sup> L. Petit, A. Svane, Z. Szotek and W.M. Temmerman, *Science* **301**, 498 (2003).
- <sup>44</sup> L. Petit, A. Svane, W. M. Temmerman, and Z. Szotek, *Phys. Rev. B* **63**, 165107 (2001).
- <sup>45</sup> P. Strange, A. Svane, W.M. Temmerman, Z. Szotek, and H. Winter, *Nature* **399**, 756 (1999).
- <sup>46</sup> M. R. Pederson, R. A. Heaton, and C. C. Lin, *J. Chem. Phys.* **82**, 2688 (1985).
- <sup>47</sup> J. G. Tobin, K. T. Moore, B. W. Chung, M. A. Wall, A. J. Schwartz, G. van der Laan, and A. L. Kutepov, *Phys. Rev. B* **72**, 085109 (2005).
- <sup>48</sup> E. Arola, M. Horne, P. Strange, H. Winter, Z. Szotek and W.M. Temmerman, *Phys. Rev. B* **70**, 235127 (2004).
- <sup>49</sup> P. Söderlind, O. Eriksson, B. Johansson, J. M. Wills, *Phys. Rev. B* **50**, 7291 (1994)
- <sup>50</sup> L. Nordström, J. M. Wills, P. H. Andersson, P. Söderlind, and O. Eriksson, *Phys. Rev. B* **63**, 035103 (2000).
- <sup>51</sup> R. C. Albers, A. M. Boring, J. M. Wills, L. E. Cox, O. E. Eriksson, and N. E. Christensen, *Phys. Rev. B* **54**, 14405 (1996).
- <sup>52</sup> A. L. Kutepov, and S. G. Kutepova, *J. Phys.: Condens. Matter* **15**, 2607 (2003).
- <sup>53</sup> N. Baclet, M. Dormeival, L. Havela, J. M. Fournier, C. Valot, F. Wastin, T. Gouder, E. Colineau, C. T. Walker, S. Bremier, C. Apostolidis, and G. H. Lander, *Phys. Rev. B* **75**, 035101 (2007).
- <sup>54</sup> J. C. Lashley, J. Singleton, A. Migliori, J. B. Betts, R. A. Fisher, J. L. Smith, and R. J. McQueeney, *Phys. Rev. Lett.* **91**, 205901 (2003).
- <sup>55</sup> J. H. Shim, K. Haule, and G. Kotliar, *Nature* **446**, 513 (2007).
- <sup>56</sup> A. Svane, N. E. Christensen, L. Petit, Z. Szotek, and W. M. Temmerman, *Phys. Rev. B* **74**, 165204 (2006).
- <sup>57</sup> T. Gouder, P. M. Oppeneer, F. Huber, F. Wastin, and J. Rebizant, *Phys. Rev. B* **72**, 115122 (2005).
- <sup>58</sup> J. R. Naegele, L. Manes, J. C. Spirlet, and W. Müller, *Phys. Rev. Lett.* **52**, 1834 (1984).
- <sup>59</sup> N. Mårtensson, B. Johansson, and J. R. Naegele, *Phys. Rev. B* **35**, 1437 (1987).
- <sup>60</sup> S. Heathman, R. G. Haire, T. Le Bihan, A. Lindbaum, K. Litfin, Y. Meresse, and H. Libotte, *Phys. Rev. Lett.* **85**, 2961 (2000).
- <sup>61</sup> P. Söderlind, O. Eriksson, B. Johansson, J. M. Wills, and A. M. Boring, *Nature*, **374**, 524 (1995).
- <sup>62</sup> B. Kanellakopulos, J. P. Charvillat, F. Maino, and W. Müller, in *Transplutonium*, edited by W. Müller, and R. Lindner (North-Holland, Amsterdam, 1975), p. 182.
- <sup>63</sup> P. G. Huray and S. E. Nave, in *Handbook on the Physics and Chemistry of the Actinides*, eds. A. J. Freeman and G. H. Lander (North-Holland, Amsterdam, 1987), vol. 5, pp. 311.



<sup>64</sup> U. Benedict, J. R. Peterson, R. G. Haire, and C. Dufour, *J. Phys. F: Met. Phys.* **14**, L43 (1984); R. G. Haire, J. R. Peterson, U. Benedict, and C. Dufour, *J. Less-Comm. Met.* **102**, 119 (1984).

<sup>65</sup> M. Lüders, A. Ernst, M. Däne, Z. Szotek, A. Svane, D. Ködderitzsch, W. Hergert, B. L. Györfy and W. M. Temmerman, *Phys. Rev. B* **71**, 205109 (2005).